Response to reviewer comments for the manuscript *Stratified suppression of turbulence in an ice shelf basal melt parameterisation*

EGUsphere-2024-3513
C.K. Yung, M.G. Rosevear, A.K. Morrison, A.McC. Hogg & Y. Nakayama
March 6, 2025

We thank the three reviewers for their thorough reading of our paper and insightful comments and feedback. We have spent time thinking about their suggestions. In particular, we have rerun the Pine Island Glacier model simulations by tuning the drag coefficient in all simulations to better compare with satellite-derived observations, and then compared the spatial distribution of melt rates between them. We hope that we have implemented the suggested changes to the satisfaction of the reviewers, but are very happy to continue discussing any aspects of the review and manuscript.

Below we respond to each comment in turn (with our responses indicated in blue) and changes that we have made to the manuscript and will resubmit if invited by the Editor. Edits to the text are written in purple, and line numbers refer to the revised manuscript.

Reviewer 1

The submitted manuscript targets a very important goal, to improve parameterized melt rates over a range of oceanographic forcings in regional-scale ice shelf-ocean models. This is certainly a worthwhile study that will eventually produce a meaningful contribution to the cryosphere science community. The present manuscript draft starts out fairly strong, but becomes cluttered and hard to follow as it progresses, making the Results Section actually quite hard to interpret based on which methodological approach was taken. There are also some holes in the approach that I have outlined as areas of improvement. While I do not believe that all of these suggested comments need to be implemented, the authors should really consider them and at least add caveats to the text for transparency. The suggested changes will constitute a major revision, but I do believe that this study worthy of eventual publication and will make a nice contribution to the cryosphere science community.
We thank the reviewer for their valuable comments that have helped to improve the manuscript, and also thank them for pointing out highly relevant literature.

Larger Comments:

1. The Introduction is quite good, but lacks some qualification on the effects of realistic small-scale slopes on ice shelf basal melting around Antarctica. Please add several sentences that play this out some. This could include some discussion of the very interesting variation in melt in a terrace, for instance.
   Thank you for the suggestion. Your comment highlighted the many different scales involved in ice shelf melting. We have added a paragraph in the Introduction discussing the various scales of ice shelf melt and ice base variation and comparing them to the much larger scales of ocean model grid sizes:

   L102-118: It is important to highlight the many spatial scales involved in ice shelf basal melting. Considering vertical resolution, the processes within the ice shelf ocean boundary layer can be less than $\mathcal{O}(10^{-3})$ m in size, hence the need for basal melt parameterisations in ocean models. Horizontally, the ice shelf base and bottom topography have significant spatial variability on scales between $\mathcal{O}(10^{-1} - 10^{3})$ m, with melt rate varying correspondingly (Nicholls

et al., 2006; Dutrieux et al., 2014; Alley et al., 2016; Watkins et al., 2021; Schmidt et al., 2023; Washam et al., 2023; Wåhlin et al., 2024). For example, in an ice base crevasse, melt rates can be enhanced at the terrace side-walls, with freezing by buoyant, supercooled water at the top of the crevasse (Washam et al., 2023), indicating multiple physical drivers of melt within a small distance. A variety of ice features such as scallops and terraces can form depending on the ice melt regime (Washam et al., 2023; Wåhlin et al., 2024). Though idealised and process models have simulated some of these small-scale features (Jordan et al., 2014; Zhou and Hattermann, 2020; Wilson et al., 2023), and some high-resolution regional models may capture part of the spatial variability (Nakayama et al., 2019, 2021; Shrestha et al., 2024), large-scale ocean models generally have horizontal grid sizes greater than $\mathcal{O}(10^3)$ m and vertical resolutions $\mathcal{O}(10^1)$ m and cannot resolve ice base variability at the required scales, nor do commonly-used bathymetry and ice base forcing products (Morlighem et al., 2020). Therefore, although there are known regions of significant ice shelf base variability and high slopes (Washam et al., 2023; Schmidt et al., 2023; Wåhlin et al., 2024), much of Antarctic ice shelves are represented in ocean models as weakly sloped ($< 1°$) from the horizontal. Quantifying the effect of small-scale ice shelf base variation on large-scale melt and optimising their representation in ocean model melt rate parameterisations requires ongoing observational and modelling work.

2. Need to define the regions of the boundary layer in the Introduction, as there are parts of the Methodology that are unclear to the reader as to which part of the boundary layer the authors are referring to.
   We have added a paragraph in the Introduction defining the boundary layer sublayers:
   L39-49: The ice shelf–ocean boundary layer is typically defined as the boundary layer formed by friction of a mean ocean flow against the ice shelf. Within this layer, there is a viscous sublayer closest to the ice, which is order mm thick and where flow is laminar (Pope, 2001). Further away from the ice, a "log" sublayer forms within which turbulence is affected by the wall boundary, and velocities scale logarithmically with distance from the ice (Pope, 2001; McPhee, 2008). Outside of this surface sublayer is the turbulent outer sublayer. The ice shelf–ocean boundary layer is affected by Earth's rotation, which sets the boundary layer depth (McPhee, 2008; Jenkins, 2016). Multiple physical processes contribute to melting beneath ice shelves in the ice shelf–ocean boundary layer. These include the molecular diffusion of heat and salt, turbulence generated by ocean currents interacting with the ice, and convective flows driven by buoyant meltwater (Malyarenko et al., 2020; Jenkins, 2021; Rosevear et al., 2024). Various parameterisations (e.g. McPhee et al., 1987; Hellmer and Olbers, 1989; Holland and Jenkins, 1999; Kerr and McConnochie, 2015; McConnochie and Kerr, 2017; Schulz et al., 2022; Zhao et al., 2024) exist to account for these processes where they cannot be resolved.

3. Methodology says very little about salinity differences, which are the key driver of stratification in the boundary layer in a warm cavity ice shelf.
   We have added a line in the methods to explicitly indicate the importance of salinity in ocean stratification in Section 2.2:
   L210-211: The stratification within Antarctic ice shelf cavities is dominated by salinity variation. Meltwater, which is relatively fresh and therefore buoyant, tends to stratify the water column.

4. Introduction should state the velocity ranges considered here before discussing friction velocity.

The friction velocity was not mentioned in the Introduction, but we presume the reviewer meant Section 2.1. We have added a line indicating these velocity ranges:
L166-167: Typical far-field velocities in ice shelves are 0.01 to 0.1 $\mathrm{m\,s^{-1}}$ (Table B1), corresponding to friction velocities of 10^{-4} to $10^{-3}\,\mathrm{m\,s^{-1}}$.

5. Consider boiling down the parameterization results to Stanton Numbers and constant Gammas, so that larger-scale models and observations that do not resolve all the way up to the ice base can implement these results into something easily useable.
Most ocean models separate transfer coefficients and drag coefficients (Asay-Davis et al., 2016), since often the drag coefficient also acts in the momentum equation. Since the transfer and drag coefficients are multiplied together in the melt parameterisation, the choice to only vary the transfer coefficient is a choice built on the results of Rosevear et al. (2022b) as discussed in Section 2.3. The intention of the parameterisation was to have varying transfer coefficients, and therefore varying Stanton numbers. In case it was confusing, we have removed a sentence that mentioned the Stanton number as a possible alternative parameterisation (since choosing to modify the transfer or drag coefficients is equivalent; what we meant was that the drag coefficient could also be modified independently or at the same time) and have instead defined the Stanton number in a more helpful place when the three-equation parameterisation is introduced.

   L178-179: Note that the thermal ($\Gamma_T C_d^{1/2}$) and haline ($\Gamma_S C_d^{1/2}$) Stanton numbers are often used to describe the combined effect of the transfer and drag coefficients.

6. Authors generally do not seek to ground their modeling in observations of the highly varied and sloping bases of Antarctica's ice shelves.
We agree with your observation and have included more mentions of this variation in our revised manuscript, including in places you have suggested (thank you!). In particular, we highlight that our models are limited by their relatively coarse horizontal and vertical resolution, so the different scales that the ocean model simulates versus the scale of the small-scale processes and features (e.g. turbulence driving melt, terraces and scalloping) are distinct, presenting a challenge for the accurate modelling of these processes in large-scale models. We have added a paragraph in the introduction to highlight this difference in spatial scales (see response to comment #1).

7. I think the authors have a real opportunity here to implement the StratFeedback+MK18 parameterization in the MITGCM Pine Island Glacier model run to take into account the external shear-driven turbulence, near-ice stratification, and the destabilizing effect rising meltwater on sloping ice bases. This will really round out the study and should test the influence of external turbulence plus localized rising plumes in a significant manner.
We did implement the StratFeedback+MK18 parameterisation in the MITgcm Pine Island Glacier simulation, which was briefly mentioned in our original manuscript but not included in our Figures. Based on your suggestion, and that of Reviewers 2 and 3, we have rerun the models but tuned them to an observation-derived baseline melt rate and compared their spatial distributions. The revised Fig. 9 and new Fig. D1 describe this, and we expand our discussion of the StratFeedback+MK18 parameterisation in Sect. 4.4. This new section is attached to the end of this response.

8. Generally, the Results Sections are hard to interpret, because it is hard for the reader to disentangle the details of which Methodology was used for each section.
Thank you for bringing this to our attention. We have tried to streamline our results section

by only showing temperature, salinity transects, melt rates and overturning streamfunctions for one model (MOM6) with the other in the Appendix, therefore decreasing the number of main text figures. We have also rearranged the results so that the first section only describes the ISOMIP+ results with prescribed tidal velocity, section 2 explores the three low-velocity limits without tides, section 3 looks at the effect of explicitly simulating tides, and section 4 is for the Pine Island Glacier analysis. We have also added signposting phrases to better indicate this division. We hope these edits improve the readability and clarity of the results section.

Abstract:

This is a long abstract that Microsoft Word registers as 257 words. Please double check that this fits within the journal's word count limit. We have revised and shortened the abstract.

Li 7: "and diffusive convection plays a role. . . " This is an unfinished statement. Please rewrite to finish this thought.

As this study focuses on improving parameterisations of the stratified regime of ice shelf melt rather than diffusive convection, we have elected to remove the mention of diffusive convection in the abstract.

Li 11 – 15: This section focuses on the suppression of melt by stratification, but does not mention the effects of diffusive convection, which is mentioned previously. Rewrite this section to add some discussion of diffusive convection.

See above response: no longer relevant.

Introduction:

Li 23: It would be helpful to add a more recent citation here on recent acceleration in melting; the latest one was over a decade ago in 2014.

We have now added citations to Paolo et al. (2015) and Rignot et al. (2019).

Li 32: While not from Antarctica, this study is very applicable to stratified ocean-driven melt of ice shelves and could be added to this list: (Washam et al., 2020). It also has to do with buoyancy-driven circulation and melt, so probably fits into the introduction well.

Washam, P., Nicholls, K. W., Mu¨nchow, A., & Padman, L. (2020). Tidal modulation of buoyant flow and basal melt beneath Petermann Gletscher Ice Shelf, Greenland. Journal of Geophysical Research: Oceans, 125(10), e2020JC016427.

Thank you for pointing out the relevance of this study. We have added it.

Li 39: I suggest to change to "the variable molecular diffusion of heat and salt"

Thanks, done.

Li 46: Should this be "turbulent mixing and heat and salt transport"

Thanks, done.

Li 50 – 54: I think somewhere in this part of the introduction or before it should be mentioned that "buoyancy-driven convection" only enhances melt along sloping ice bases, and that the growing number of observations from beneath ice shelves show that their bases' are quite rough with many slopes.

Thank you, we have added this.

L60-62: The parameterisation also does not account for buoyancy-driven convection that may enhance melt along sloped ice bases (e.g. McConnochie and Kerr, 2017), with significant ice base slopes recently observed beneath Antarctic ice shelves (e.g. Washam et al., 2023; Wåhlin et al., 2024), or the effect of diffusive convection....

Li 70: Please add one or both of the following citation to the statement that variation in melt rate within each ice shelf is significant: (Vaňková and Nicholls, 2022; Vaňková et al., 2023).

Vaňková, I., & Nicholls, K. W. (2022). Ocean variability beneath the Filchner-Ronne ice shelf inferred from basal melt rate time series. Journal of Geophysical Research: Oceans, 127(10), e2022JC018879.

Vaňková, I., Winberry, J. P., Cook, S., Nicholls, K. W., Greene, C. A., & Galton-Fenzi, B. K. (2023). High spatial melt rate variability near the Totten Glacier grounding zone explained by new bathymetry inversion. Geophysical Research Letters, 50(10), e2023GL102960.

Added, thank you for the suggestion.

Li 87: This statement is way oversimplified and should be removed: "whereas Antarctic ice shelves are generally weakly sloped (<1°)". There are a growing number of observations that show this is not the case over many scales, from scalloped morphology (<1 m) to a several km grounding zone.

We have removed the statement. Our intention with this statement was in reference to the large-scale slopes resolved by an ocean model (e.g. from BedMachine v3 data, which has a resolution of 500 m). As mentioned in response to major point 6, we have expanded our introduction to discuss ice base slopes in Antarctica, including small-scale, high-slope features as seen in recent work and their distinction from large-scale, low-slope features resolved by ocean models. We have also rephrased the statement in question to refer specifically to the Ross Ice Shelf borehole observation used in the Malyarenko et al. 2020 analysis as

L94-98: Some of these parameterisations match well with *in situ* observations, such as the Kerr and McConnochie (2015) parameterisation which captures convective melt rates at vertical ice faces in Greenland (Schulz et al., 2022; Zhao et al., 2024) and beneath Ross Ice Shelf (Malyarenko et al., 2020). The latter is notable since the Kerr and McConnochie (2015) laboratory study uses vertical ice faces whereas the studied region of the Ross Ice Shelf is weakly sloped ($< 1°$)from the horizontal (Stewart, 2018; Malyarenko et al., 2020).

Melt Parameterisation Design and Validation:

The Three-Equation Melt Paramterisation and Transfer Coefficients

Li 127: I would say the ice-ocean boundary temperature is also a key unknown, but if you solve the three equations Tb and Sb will drop out through the quadratic expression. Perhaps you can add some discussion on this to this section, which is typically glossed over in papers. This could also be added to the Li 132.

Sorry for the confusion, we meant that the transfer coefficient is a key unconstrained parameter, not an unknown of the system of equations. We have replaced this phrase with

L155: "The key unconstrained parameter here that must be chosen according to empirical values or theory is the transfer velocity for heat..."

and added to our explanation for the unknowns in the system of equations:

L160-162:"These three equations (1-3) are solved to obtain the three unknowns; the salinity S_b

and temperature T_b at the ice-ocean interface, and the melt rate m. If the transfer coefficient is independent of these three unknowns, this system of equations reduces to a quadratic equation."

Li 140: Also an opportunity to cite the Washam et al. (2020) paper.

We have added this citation as well as a few others.

L169-173: The values of these transfer coefficients are not well known: they can be tuned to observed estimates, as Jenkins et al. (2010) (hereafter J10) did at the Filchner-Ronne ice shelf using co-located borehole ocean measurements and radar-derived melt rates (and others, e.g. Davis and Nicholls, 2019; Washam et al., 2020; Rosevear et al., 2022a; Davis et al., 2023, have done elsewhere) or tuned in an ocean model to give a desired melt rate (Asay-Davis et al., 2016; Nakayama et al., 2018; Hyogo et al., 2024).

Li 146 – 151: Again, this is focused on flat portions of the ice shelf and requires a qualifying statement that sloped ice can melt faster that the J10 and HJ99-M81 parameterizations, e.g., Schmidt et al., (2023).

We added

L187-188: Significant basal slopes can also contribute to deviations from the shear-driven J10 and HJ99-M81 parameterisations (Schmidt et al., 2023).

Li 148: I think it would be helpful to add the M81 stability parameter as an equation, so that the reader can be compare it with (5) in the following discussions. I do see it later in the Appendix, but it may help to have it in the main body or at least reference that it is in the Appendix.

We decided to simply reference that it is in the Appendix to avoid duplicate definitions of variables.

L177: see Eqn. A5 for the stability parameter definition

Li 151 – 160: Please include a discussion of Washam et al., (2023) and Lawrence et al., (2023) in this section on drag coefficients, as both studies quantified ice shelf morphology and related them to a u* and CD from observations.

Washam, P., Lawrence, J. D., Stevens, C. L., Hulbe, C. L., Horgan, H. J., Robinson, N. J., ... & Schmidt, B. E. (2023). Direct observations of melting, freezing, and ocean circulation in an ice shelf basal crevasse. Science Advances, 9(43), eadi7638.

Lawrence, J. D., Washam, P. M., Stevens, C., Hulbe, C., Horgan, H. J., Dunbar, G., ... & Schmidt, B. E. (2023). Crevasse refreezing and signatures of retreat observed at Kamb Ice Stream grounding zone. Nature Geoscience, 16(3), 238-243.

We have added:

L193–196: Most suggested values range from 0.0015 (Holland and Jenkins, 1999) to 0.0097 (Jenkins et al., 2010), with a value of 0.0022 estimated from turbulence measurements beneath the smooth underside of Larsen C Ice Shelf (Davis and Nicholls, 2019) and 0.0036 estimated from basal ice morphology beneath the crevassed Ross Ice Shelf grounding zone (Lawrence et al., 2023).

and

L200-201: Additionally, Washam et al. (2023) find an order of magnitude of spatial variation in drag coefficient within a single ice shelf basal crevasse.

Stratification Feedback on Turbulence – Insights from Large Eddy Simulations:

Li 161 – 167: This paragraph never mentions salinity, which is the principle driver of density at the ocean temperatures responsible for melting ice shelves. Please properly attribute stratification to difference in density, driven by salinity changes. Additionally, and potentially more important, this discussion only applies to flat or gently-sloping ice where meltwater pools instead of rises vigorously to act as a source of turbulence that destratifies the boundary layer. This must be said in this paragraph also.

As mentioned in major point #3, we have added a sentence highlighting the importance of salinity in stratification. We have also clarified that the stratification effect we discuss applies to flat or weakly sloped ice shelves:

L207–209: The other is the ability of stratification to suppress boundary layer turbulence beneath horizontal or gently sloping ice shelves (noting that the same turbulence feedback may not apply beneath steeply sloped ice bases where meltwater can drive buoyant flow up-slope, generating turbulence).

and emphasise the LES simulations looked at horizontal and weakly sloped ice bases:

L212–213: Vreugdenhil and Taylor (2019) and Rosevear et al. (2022b) use Large Eddy Simulations (LES) beneath horizontal and weakly sloped ice bases to diagnose regimes of Antarctic ice shelf melt.

Li 173: Does a small L+ here refer to an absolute sense or a highly negative value? This is slightly non-intuitive, since there is a negative in front of u* in (5), g is a positive 9.80 m/s2, and one might expect Tb – TM to be larger (more negative) than Sb – SM, which would result in a positive buoyancy flux. Please spell this out for the reader, or preferably, move the expressions around in the 3 equation parameterization to place a positive sign in front of the heat/salt flux and make it TM - Tb (SM – Sb), then place a negative sign in front of the heat conduction into the ice shelf.

We focus only on positive values as the destabilising buoyancy flux parameter space has not been tested by the LES simulations we use. We have added a line to clarify this:

L220–221:We focus only on positive values of L^+, indicating a stabilising (negative sign) buoyancy flux; the LES simulations do not explore freezing and destabilising conditions.

We have also rearranged Eqns. 2 and 3 as suggested.

We don't think it is possible (if heat conduction is neglected) for melting conditions to result in a destabilising flux (i.e. $\alpha(T_M - T_b) > \beta(S_M - S_b)$). Note $\beta/\alpha \sim 20°\text{C}/(\text{g/kg})$ in ice shelf cavity conditions so a destabilising flux with $T_M > T_b$ and $S_M > S_b$ would require $T_M - T_b > 20(S_M - S_b)°\text{C}/(\text{g/kg})$. Rearranging Eqns. 2 and 3,

$$\frac{T_M - T_b}{S_M - S_b} = \frac{\gamma_S L_f}{\gamma_T C_p S_b} \tag{1}$$

and with $\gamma_S/\gamma_T \sim 1/35$, $L_f/C_p \sim 80$ °C and $S_b \sim 30$g/kg this leaves the RHS approximately $\frac{1}{15}°\text{C}/(\text{g/kg})$, clearly not large enough to cause a destabilising flux. We have highlighted the importance of the salinity in the buoyancy flux here:

L222-223: Note $\beta/\alpha \sim 20\,°\text{C}\,/(\text{g}/\,\text{kg})$ in ice shelf cavity conditions (Asay-Davis et al., 2016) so salinity changes control the buoyancy flux.

Li 173: Is this kinematic viscosity or eddy viscosity?

It is molecular viscosity. We have made this explicit.

Li 189 – 190: I do not understand how the cooling effect of melting is not accounted for in L+, since the buoyancy term (Bb) should exhibit some change in TM and SM as the boundary layer cools and freshens from melting. Unless TM and SM are chosen at a sufficient distance to be truly "far-field." To be honest, I have a hard time understanding where TM and SM are chosen in most papers. Please elucidate this more clearly in this section.

In ocean models, far-field temperatures and salinities, T_M and S_M, are typically averaged over the mixed layer or top-most grid cell, order 10 m or larger (Asay-Davis et al., 2016; Gwyther et al., 2020). In the borehole observations tested in Fig.3, generally far-field temperatures are also taken ∼10 m from the ice. Thus, far-field temperatures may not generally capture the boundary layer cooling. We have added some more words to clarify this:

L205–207: Stratification due to buoyant meltwater has two distinct effects on the melt rate. One is the effect of meltwater to cool and freshen the surface boundary layer, which decreases the relevance of the far-field temperature that parameterisations generally consider (Rosevear et al., 2022b) as a heat source for melting.

L237–239: In contrast, the Rosevear et al. (2022b) stratified regime definition includes the effect of stratified meltwater to cool the boundary layer relative to the far-field temperature as mentioned earlier, which is not captured by L^+.

Stratification Feedback Parameterisation Design:

Li 194: Add "along flat or gently-sloping ice to the end of this sentence."

Done, thank you.

Li 205 – 207: Briefly comment on how neglecting the heat conductive flux will influence results, citing literature that has considered this variable, e.g., Arzeno et al. (2014), Washam et al. (2020), and others. Note that importantly at low ocean heat fluxes, the conductive heat flux through the ice shelf can be nearly as high as the ocean heat flux, which plays an important role in transitioning from melting to freezing.

Arzeno, I. B., Beardsley, R. C., Limeburner, R., Owens, B., Padman, L., Springer, S. R., ... & Williams, M. J. (2014). Ocean variability contributing to basal melt rate near the ice front of Ross Ice Shelf, Antarctica. Journal of Geophysical Research: Oceans, 119(7), 4214-4233.

Thank you for pointing this out. We ran brief tests with the conductive flux (the recommended linearised advection-diffusion form of Holland and Jenkins (1999)) turned on in MOM6, and mean melt rates were less than 10% smaller (Fig. R1), so we do not expect the results to vary qualitatively with conductive heat flux included. Holland and Jenkins (1999) also suggest a similar 10% change.

We have added the following comment:

L257–261: Note that we also neglect the conductive heat flux term of Eqn. **??**; although the conductive heat flux may be an important term in some ice shelf cavity conditions (Holland and Jenkins, 1999; Arzeno et al., 2014; Washam et al., 2020; Wiskandt and Jourdain, in review), melt rates are not expected to decrease by more than 10% (Holland and Jenkins, 1999). Thus, we do not expect qualitatively different conclusions when we omit the conductive heat flux term.

Li 211 – 212: The velocity in the boundary layer should be less than far-field, because the

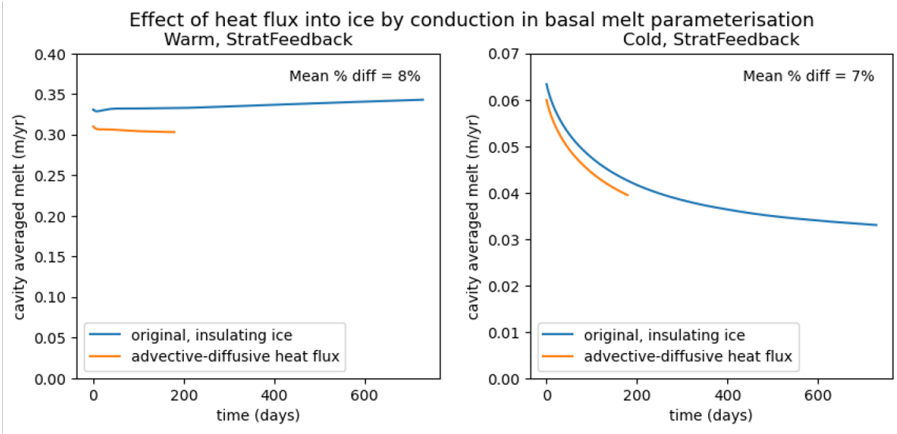

Figure R1: Effect of heat conductive flux in MOM6 ISOMIP+ with insulating ice (no heat flow into ice, $Q_I^T = 0$) in blue and conducting ice (with the linearised advection-diffusion form of Holland and Jenkins (1999) (option C of Wiskandt and Jourdain, in review) in orange. Left panel shows the warm experiment and right the cold. The StratFeedback parameterisation is used with ISOMIP+ protocol of prescribed tidal velocity (i.e. $U_{tide} = 0.01\,\mathrm{m\,s^{-1}}$).

oceanic flow is starting to feel the friction of the ice base, which generates turbulent eddies that mix heat and salt towards the ice. There are also multiple regions of the boundary layer, such as the outer, surface, and viscous sublayer, that have not been properly defined at this point (see general comment). All of this needs to be spelled out clearly to the reader, and sentences like this are presently confusing, because the boundary layer has not been properly introduced.

As discussed in response to major comment #2, we have added the boundary layer definitions to the Introduction. We also modified this sentence, also in response to reviewer 3:

L267: Monin-Obukhov theory expects that under a stabilising buoyancy flux, the drag coefficient is also reduced as the friction velocity is suppressed relative to a fixed far-field velocity (the drag coefficient is defined as the ratio of these speeds).

Li 216 – 217: If the whole domain is laminar, then there is no turbulence, right? Then if the drag coefficient is related to the friction velocity and therefore turbulence, how can there be a drag coefficient if there is no turbulence? I realize that this is a literature review, but I think this should be presented more clearly to the reader.

Your comment highlighted that the drag coefficient is not particularly meaningful for the intermittently laminar case in Vreugdenhil and Taylor (2019). We have simplified and clarified the text which justifies our use of a constant Cd on the basis of the results of Rosevear et al. (2022b).

L266–274: We could also consider an alternative parameterisation where the drag coefficient, as well as the transfer coefficients, is varied. Monin-Obukhov theory expects that under a stabilising buoyancy flux, the drag coefficient is also reduced as the friction velocity is suppressed relative to a fixed far-field velocity (the drag coefficient is defined as the ratio of these speeds). Indeed, Vreugdenhil and Taylor (2019) see a reduction in the drag coefficient in LES experiments with smaller L^+. However, Rosevear et al. (2022b) do not see a systematic variation in drag coefficient with L^+ (Fig. 1d). The difference in the behaviour of the drag coefficients between the LES studies, which otherwise agree strongly, is likely due to the different methods of forcing the current beneath the ice. We assume the approach of Rosevear et al. (2022b), which involves forcing the model domain with a steady, far-field flow in geostrophic balance and allowing an

Ekman boundary layer to form, to be somewhat more realistic. We therefore choose to follow the data of Rosevear et al. (2022b) in Fig. 1d, and keep the drag coefficient constant in our study. Note that changing C_d would also change the surface boundary drag law parameterisation in some models.

Li 221: Please change to vary the thermal and haline Stanton numbers ($\Gamma_T((C_D)^{1/2})$ and $\Gamma_T((C_D)^{1/2})$)

Done.

Li 223 – 228: This sentence suggests that the authors are solving the two-equation parametrization, where there is a salinity difference across the boundary layer of 0. I don't think this is actually the case, but it would be helpful for the authors to clarify this in the text.

Thank you for picking up this confusion. The thermal driving metric, $T_M - T_{fr}(S_M)$ used in the plots differs from the thermal driving term in the three-equation parameterisation $T_M - T_{fr}(S_b)$. Though we use the latter in the calculation of melt rates, we chose to plot the former since it is easier to calculate, particularly for observations, and it is independent of transfer coefficient so allows for easier comparison of parameterisations. $T_M - T_{fr}(S_M)$ quantifies the maximum amount of heat available rather than the actual heat delivered due to changes in the freezing point with salinity. We have made this clear in the text.

L281–284: Note this thermal driving may be smaller than the actual temperature difference delivering heat from the ocean for melting that we computed using the three-equation parameterisation ($T_M - T_b$ in Eqn. 2), but is independent of transfer coefficient choices and therefore more appropriate when comparing parameterisations.

Li 223 – 239: I believe that it is roughly an order of magnitude greater, but it would be helpful to just state the actual far-field velocity range that could produce u* values of 0 – 0.010 m/s.

We added

L293: At a thermal driving of $T^* = 2°C$ and $u_* = 0.001\ \mathrm{m\,s^{-1}}$ (far-field velocities of $\sim$2 cm/s, on the lower end of observed speeds; Table B1)

Comparison to Observations:

Li 241 – 260: See comment on Figure 3 below also. Please add Ross Ice Shelf data from Washam et al. (2023) to these plots. While not Antarctica, it may also be helpful to place the detailed data from Petermann Glacier into this discussion.

Washam, P., Lawrence, J. D., Stevens, C. L., Hulbe, C. L., Horgan, H. J., Robinson, N. J., ... & Schmidt, B. E. (2023). Direct observations of melting, freezing, and ocean circulation in an ice shelf basal crevasse. Science Advances, 9(43), eadi7638.

Washam, P., Nicholls, K. W., Mu¨nchow, A., & Padman, L. (2020). Tidal modulation of buoyant flow and basal melt beneath Petermann Gletscher Ice Shelf, Greenland. Journal of Geophysical Research: Oceans, 125(10), e2020JC016427.

Thank you for the suggestions. We have looked through these papers but feel it would be inconsistent to add them to Figure 3. Our criteria for including studies in this figure was that studies should have a co-located radar-derived melt rate and profile of ocean conditions, including measured far-field temperature, salinity and velocity so that they can be compared in Fig.3a. To the best of our knowledge, Washam et al. (2020) does not directly measure velocities, which are instead inferred from a tuning between meltwater pulse time-lags between different

sites on the same glacier and the use of a melt parameterisation. Whilst Washam et al. (2023) does directly measure velocities, we could not find co-located radar measurements of melt rate. Washam et al. (2023) could technically be added to panel b of the figure. However, our intent in this figure is to show the regimes associated with the comparison of co-located radar-derived and parameterisation-derived melt rates, rather than provide a complete overview of the observed ice shelf–ocean boundary layer regimes around Antarctica and Greenland (which would add many other studies and is a great suggestion for future work!) so we would prefer to retain the figure as is. We have ensured these studies are mentioned elsewhere in the manuscript. To clarify our criteria, we added:

L298-299: Following Rosevear et al. (2022a), we compare the melt rate produced by the Strat-Feedback and ConstCoeff melt parameterisations using limited direct observations of borehole ocean conditions and co-located, direct melt rate measurements in Antarctic ice shelves.

Li 248: I would be careful to say that ignoring heat conduction makes no difference on melt rate parameterization at low ocean heat and salt fluxes, i.e., cold cavity conditions.

We have modified our statement to weaken it (and to emphasise that we don't expect the fact that the overestimation will change, even if the melt rates themselves do change), see also Figure R1 and response to L205-207 demonstrating a minor change in melt rate.

L303–305: recall we ignore heat conduction into the ice, but these choices are not expected to qualitatively change the overestimation of melt rates.

Limiting to a Velocity-Independent Parameterisation:

Li 266: Following the comment above, it would be helpful to define what velocity range constitutes "low-velocity."

We have defined it to be far-field flows of 1 cm/s or smaller, since this is the scale of the ISOMIP+ prescribed tidal velocity:

L323–325: There is both a numerical and physical reason for the low-velocity ice shelf cavity regime to be specially treated with the three-equation parameterisation (where this regime is characterised by low velocities, here taken as far-field flows of $1\,\mathrm{cm\,s^{-1}}$ or smaller, but has considerable overlap with the $L^+ < 2500$ diffusive-convective regime).

Li 274 – 275: Thank you for identifying the varying ocean-forced mechanism that relate to differing ice slopes.

Thanks.

Li 299: turbulent or molecular diffusion? If molecular, then the sublayer thickness will need to be accounted for and the temperature and salinity gradient across it. If turbulent, please explain this further. Is it just a really low U multiplied by sqrt(C_D)?

Molecular diffusion. However, we cannot resolve these processes in an ocean model, so this choice is a simplification used as a somewhat arbitrary parameter in some ocean models (e.g. Gwyther et al., 2016). We have added a clarification:

L363–365: where the minimum velocity is intended to represent heat transport occurring through molecular diffusion even at very low current speeds (Gwyther et al., 2016). Using a minimum velocity is a simplification for models that do not resolve the boundary layer, and this velocity does not account for the true viscous sublayer thermodynamics.

Li 266 – 306: I see no discussion of a combined StratFeedback+MK18 in this section, but (I think) this is most likely what happens in the real world along sloping ice shelf bases and I

see it in Figure 2. I suggest to add a few sentences that discuss this parameterization to this section.

Thanks for the suggestion. We added some sentences.

L372–377: Each choice of transfer and drag coefficient can be combined with each choice of low-velocity limit. In particular, the StratFeedback+MK18 parameterisation is intended to best represent real ice shelf–ocean regimes, since it encompasses the commonly used shear-driven melt parameterisation in well-mixed, shear-driven conditions, the stratified suppression of turbulence observed and suggested by LES simulations, as well as a lab-based velocity-independent convective parameterisation when far-field flows are weak. We also assess the sensitivity to the choice of low-velocity regimes with a fixed transfer coefficient parameterisation choice.

Model Configurations

ISOMIP+ Setup and Modifications

Li 324 – 325: I do not think that the cold cavity setup is restored to a very realistic T/S profile. It is fine to take a full isothermal temperature profile to represent deep convection, but if that is the case, then the salinity profile should also be nearly uniform. In any case, the choice of a surface salinity of 33.8 g/kg seems too fresh if all the freshening is to be accounted from ice melt. Take a look at hydrographic sections in front of the Ross and Filchner-Ronne and adjust accordingly. It doesn't have to be perfect, but I suggest a lower salinity range.

This is a good point and we agree that the cavity conditions in the cold ice shelf is not very realistic. We chose to use the ISOMIP+ protocol conditions mainly because it is a standard test case and therefore comparable to other models and studies, e.g. Gwyther et al. (2020). We also expect to make the same conclusions even with a more realistic cold cavity stratification profile, namely that the parameterisation is regime dependent and that cold ice shelves are in a higher L^+ regime than warm ones. For simplicity, we would like to keep the hydrography as is, but have added a caveat mentioning the unrealistic profile.

L397-399: Note these temperature and salinity profiles are highly idealised, and the cold configuration is unrealistically fresh compared to conditions within and outside the Ross and Weddell Sea ice shelves (Orlanski, 1976; Nicholls et al., 2004; Darelius et al., 2014).

Li 329: Please consider adding in the heat conduction term to these models, as it will become important in the cold cavity, low heat/salt flux scenarios, especially when the ice draft is thin. If this is not possible, remark on this as a weakness of this experiment and discuss the caveats.

It would be very time-consuming for us to run all of the configurations (44 of them) again with the heat conduction term, therefore we wish to keep the simulations as is assuming an insulating ice shelf. Additionally, the lack of heat conduction term matches the ISOMIP+ protocol, providing better comparison to other models and studies (e.g. Gwyther et al., 2020). As mentioned in response to the Li 205-207 comment, we have run the models briefly with a conduction term and saw only small ($< 10\%$) differences. We have added a caveat in the text.

L403–404: To simulate basal melt, we use the three-equation parameterisation (Eqns. 2-4) without the ice heat conduction term (noting melt rates would decrease by $\sim$10% if this term were to be included).

Idealised MOM6 Configuration

LI 335 – 349: Please explicitly mention the uppermost layer vertical grid cell size range here and remark on how well it represents observations of the boundary layer beneath ice shelves.

These models do not resolve the ice–ocean boundary layer structure, generally just having one or two cold layers near the surface.

L425-426: This vertical resolution is insufficient to resolve the structure of the ice shelf–ocean boundary layer, though the uppermost layers exhibit cooling and freshening in response to melting.

Idealised MITgcm Configuration

Li 351 – 3558: Similarly, remark on whether the 5 m partial grid cell can adequately resolve the boundary layer.

Similarly to above.

L436–437: As in MOM6, this vertical resolution is insufficient to resolve the structure of the ice shelf–ocean boundary layer.

Idealised Explicit Tidal Forcing:

Li 360 – 372: Do these tides pass the critical M2 latitude in your simulations? Is this included?

Thank you for picking up our omission. The idealised ISOMIP+ simulations are on an $f-$plane at latitude 75°S, therefore south of the M2 critical latitude. We have added a clarification of the f-plane to the methods:

L400–402: Unless specified, we follow the mixing, viscosity and equation of state protocols of ISOMIP+ (Asay-Davis et al., 2016). This protocol includes the f-plane approximation with a latitude of 75°S.

We have also commented on the critical latitude when the tidal forcing is introduced:

L445-447: Since the ISOMIP+ simulations are on an f-plane with latitude 75°S (Asay-Davis et al., 2016), the whole domain is effectively south of the M2 critical latitude (Makinson et al., 2006).

Li 370 – 372: Do these decreased tidal velocities represent observations, e.g., Jenkins et al. (2010) or Davis & Nicholls (2019)? I don't think so. Please remark on why this is the case.

Our result of weaker tidal velocities at depth beneath the ice is supported by several modelling studies: Mueller et al. (2012), Gwyther et al. (2016) and Jourdain et al. (2019) all see weaker tidal velocities near the deep grounding lines of ice shelves. To the best of our knowledge, the observational papers by Jenkins et al. (2010) and Davis & Nicholls (2019) don't explore spatial distributions of tidal velocities along the ice draft. We have added references to the modelling papers:
L450-452: However, the resulting tidal velocity at the ice-ocean interface is lower near the grounding line compared to the ice front (Fig. S1), as seen in other modelling studies (Mueller et al., 2012; Gwyther et al., 2016; Jourdain et al., 2019)

Pine Island Glacier Configuration:

Li 388 – Li 390: I highly recommend adding in the StratFeedback+MK18 parameterization to this study, as you are now dealing with a (somewhat) realistic model configuration that will experience external shear-driven turbulence, stratification, and rising meltwater plumes. This would really take this study over the top!

Thank you for the suggestion. The StratFeedback+MK18 parameterisation was included in the original manuscript but not highlighted. We have now devoted more time to it and included it in the revised Fig. 9 and Fig. D1, and analysed its spatial distribution compared to other parameterisations when tuned to satellite melt rates. The revised section is copied at the end of the document.

Results:

Idealised ISOMIP+ Results:

Li 396 – 398: Add a similar discussion on salinity differences, which are the primary driver of stratification (last time I say this), and see comment below on Figure 4.

Thank you, we have included salinity profiles in the figure as suggested and written:

L486–488: The salinity stratification, which dominates the density, is similar between warm and cold experiments with a fresh meltwater layer most prominent in Fig. 4e, though the warm experiment has saltier deep water following the ISOMIP+ protocol.

Li 408 – 414: Perhaps this can wait until the Discussion Section, but I think L+ could be artificially low in these simulations, because of the course grid size. Consider adding a section that explicitly discusses how vertical resolution affects L+ and compare it to either high resolution model runs or observations to properly ground these results.

We agree and have expanded our existing discussion in the Discussion section:

L486–493: Our results demonstrate the importance of testing basal melt parameterisations across various ice shelf cavity regimes. The basal melt-ocean circulation positive feedback makes idealised models extremely sensitive to specific choices in the parameterisation, possibly more so than realistic models. Still, achieving the expected L^+ suggested by *in situ* borehole observations, where many locations had conditions with $L^+ > 10^4$ (Fig. 3b), required large drag coefficients in the Pine Island Glacier experiment. Ocean models may not simulate true ice shelf melt regimes since they lack the small-scale flow variability observed at high frequencies beneath ice shelves, either through not resolving these scales of motion (through both horizontal and vertical resolution), or may have anomalously smooth bathymetry and ice base shape.

L696–698: This compensation, however, would be expected to depend on resolution; future research should investigate the model grid resolution dependence of simulated ice shelf regimes.

Li 429: Suggest to not cite manuscripts in preparation.

Yes, this was just a placeholder. We have removed the citation but will add it back if submitted before the present manuscript is accepted.

Sensitivity to the Low-Velocity Limit:

431: Wait, were tides included in all of the results from the previous section? If so, it was not clear to the reader, so please restate it in that section. Later in Li 439 I see that it is fully thermohaline. Please make this clearer.

They were not included. We have added some lines to signpost this.

Sec 4.1 first paragraph

L380–482: In this first section, we follow the ISOMIP+ protocol and use the low-velocity limit with a prescribed tidal contribution of $U_t = 0.01\,\mathrm{m\,s^{-1}}$ to the friction velocity (Table 2). Here, the simulations do not include explicit tides.

Sec 4.2 first paragraph

L522: In this section, we explore this sensitivity, noting as in Sect. 4.1 the simulations analysed do not include explicit tides.

Energetic Ice Shelf Cavity Regimes:

Li 460 – 491: This section should evolve after the appropriateness of L+ in these simulations has been assessed following the prior comment (Li 408 - 414). Or, this can wait to the discussion section.

We have moved part of this comment to the discussion section, and modified the rest of it here to read:

L582–586: However, the idealised tidal simulations demonstrate the difficulty in achieving realistic ice shelf cavity regimes in idealised models. Even with a large tidal forcing of $0.2\,\mathrm{m\,s^{-1}}$ amplitude velocity (corresponding to a 6.4 m sea level anomaly forcing in this idealised cavity), the warm cavity is not entirely in the well-mixed regime, possibly associated with the smoothness of the geometry and insufficient spatial resolutions.

Realistic Pine Island Glacier Simulation:

Li 493 – 532: I highly suggest to also implement the StratFeedback+MK18 parameterization into this analysis, i.e., a parameterization that includes the influence of ice base slope, stratification, and external turbulence.

Thanks for the suggestion, as mentioned in response to Li 388 comment, we have revised this analysis and section, copied at the end of the document.

Li 521 – 524: If I understand this right, this was hardly a 'tuning' of the drag coefficient and more of picking a single observed drag coefficient and applying it to the whole model. At this point it is quite difficult to follow what method has been used where. Regardless, I would not refer to this as a 'tuning,' but instead an 'altering' of the drag coefficient, then please state explicitly in this section what CD was changed from and to. I also took a look back at the Stanton et al. (2013) paper and don't see a value for CD, but instead only a timeseries of u* without any mention of U. How as CD computed then? Another approach to this problem would be to use the range of CD values observed beneath ice shelves and force the model with each of them to see how it influences the melt rates.

In the original manuscript, C_d for the benchmark, HJ99-neutral parameterisation (Nakayama et al., 2021) was taken as 0.0015 as suggested by Holland and Jenkins (1999) and used everywhere in the domain. We did not find (nor use) a C_d value from Stanton et al. (2013). The constant C_d was increased for the tuned StratFeedback simulation to 0.0042 to achieve the same mean melt rate as HJ99-neutral with C_d=0.0015 (average melt rates to within 0.1 m/yr, determined by trial and error with different choices C_d).

In our revision, also in response to Reviewers 2 & 3, we have tuned the drag coefficient for three parameterisation options (HJ99-neutral, StratFeedback+ustarmin and StratFeedback+MK18 to achieve the same area-averaged melt rates as Adusumilli et al. (2020) and compared their spatial distributions. The revised section is copied at the end of the document.

Discussion:

Li 534 – 572: All of this reads more like a Summary than a Discussion and should be rewritten to provide more helpful analysis of the results.

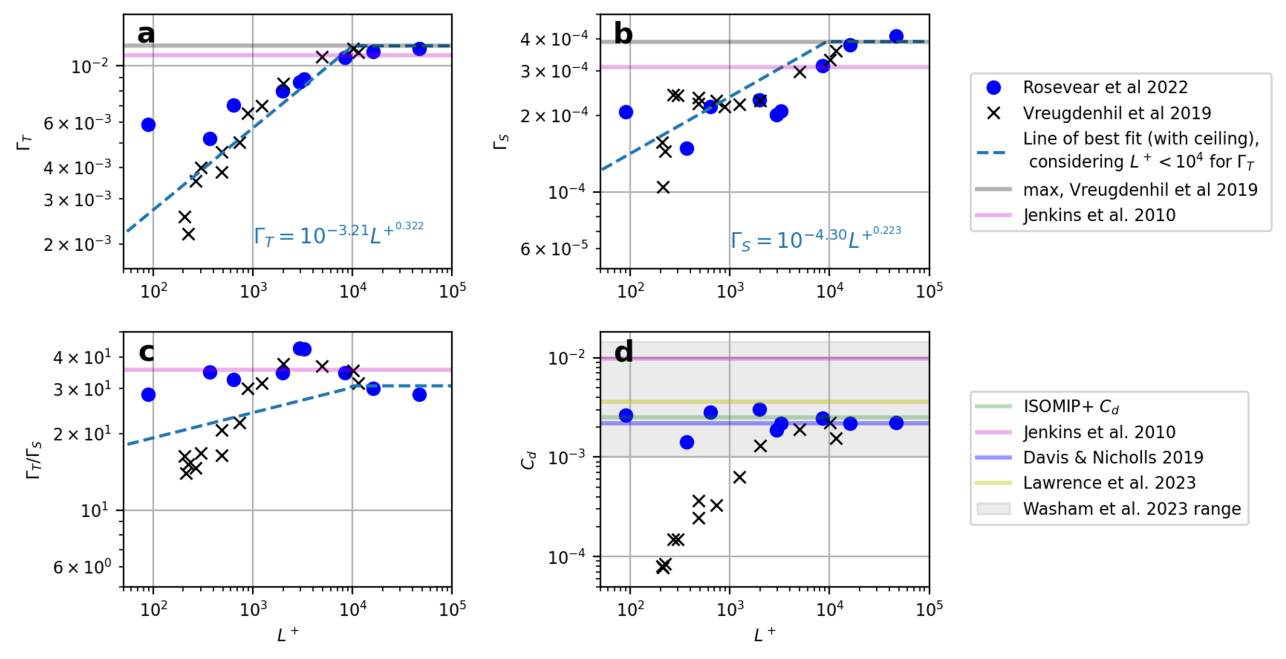

Figure R2: Large Eddy Simulation data, with Vreugdenhil and Taylor (2019) in the black crosses and Rosevear et al. (2022b) in blue dots, indicating the relationship between transfer coefficients (a) Γ_T, (b) Γ_S, their ratio (c) Γ_T/Γ_S and (d) drag coefficient C_d against viscous Obhukov scale L^+. The maximum Vreugdenhil and Taylor (2019) (ConstCoeff) values of the transfer coefficients are included (grey lines), which are similar to the Jenkins et al. (2010) values (pink lines). The blue dashed line indicates the choice of fit of transfer coefficients as a function of viscous Obukhov scale for our stratification feedback parameterisation. Drag coefficients from observations of Jenkins et al. (2010), Davis and Nicholls (2019), Lawrence et al. (2023) and Washam et al. (2023) are also included.

We have edited the Discussion to reduce the summary content, but still feel a short summary is helpful.

Li 573 – 585: Ok, this somewhat satisfies my prior comments on the validity of L+ in these simulations, but given (what I think is) the goal of this study to more accurately parameterize melt rates, I think this section should be expanded to include model-obs comparisons or coarse-fine model comparisons.

Thank you for the suggestion. We feel that it is beyond the scope of this already lengthy study to investigate the resolution-dependence of the models, so we have added a prompt for future research:

L697: Future research should investigate the model grid resolution dependence of simulated ice shelf regimes.

Figures:

Figure 1d: Consider adding lines for CD from more observations beneath ice shelves, such as Jenkins et al. (2010), Davis and Nicholls (2019), Washam et al. (2023), and Lawrence et al. (2023).

Thanks for the suggestion, we have done this. See Fig. R2.

Figure 2b: Consider adding a range of ice base angles (4 or 5 angles between 10° and 90°) to this

figure or to the Appendix, since 10° seems to be somewhat arbitrary and low, without any real acknowledgement of the many small-scale slopes observed beneath ice shelves, e.g., Dutrieux et al. (2014), Schmidt et al. (2023), Lawence et al. (2023), Washam et al. (2023), etc...

Dutrieux, P., Stewart, C., Jenkins, A., Nicholls, K. W., Corr, H. F., Rignot, E., & Steffen, K. (2014). Basal terraces on melting ice shelves. Geophysical Research Letters, 41(15), 5506-5513.

We have added figures with three angles to the Appendix A as suggested, reproduced here in Fig. R3:

Fig. A2 presents alternative angle options to the 10° slope used in Fig. 2b and Fig. A1d.

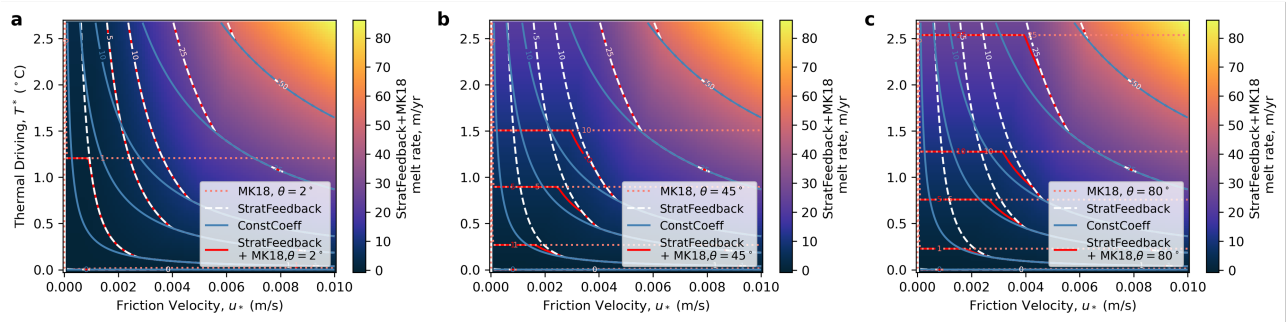

Figure R3: Thermal driving – friction velocity parameter space diagram indicating melt rates calculated as a function of far-field temperature, salinity and pressure (which are set to $S = 34.5$ psu and $p = 500$ dbar) and friction velocity. The melt rates are solved for a variety of parameterisation options: ConstCoeff is in the blue solid lines, and StratFeedback is shown in white dashed lines. Constant melt rates obtained from slope-dependent McConnochie and Kerr (2018) convective parameterisation are in the pink dotted lines, and the combination of the StratFeedback+MK18 limit is in the red dash-dot line. The three panels show different slope angle choices to Fig. 2b, with angles from the horizontal of (a) 2°, (b) 45° and (c) 80°.

Figure 3: Please add Ross Ice Shelf data from Washam et al. (2023) to these plots. While not Antarctica, it may also be helpful to place the detailed data from Petermann Glacier into this figure.

Washam, P., Lawrence, J. D., Stevens, C. L., Hulbe, C. L., Horgan, H. J., Robinson, N. J., ... & Schmidt, B. E. (2023). Direct observations of melting, freezing, and ocean circulation in an ice shelf basal crevasse. Science Advances, 9(43), eadi7638.

Washam, P., Nicholls, K. W., Münchow, A., & Padman, L. (2020). Tidal modulation of buoyant flow and basal melt beneath Petermann Gletscher Ice Shelf, Greenland. Journal of Geophysical Research: Oceans, 125(10), e2020JC016427.

Please see our response to Li 241-260.

Figure 4: I suggest to add two rows that are similar to a-h, but present Salinity.

We have done this, and removed the kinetic energy plots, combining the overturning stream-function with the other diagnostics. In response to Reviewer 2, we now only show MOM6 results in the main text and have moved the MITgcm plots to the Appendix. The updated MOM6 figures is shown in Fig. R4.

Figure 7: Given that there have been scalebar changes in the comparison of cold and warm cavities in Fig 4 and 6, I suggest to change the vertical axis in panel b and use lower melt rate

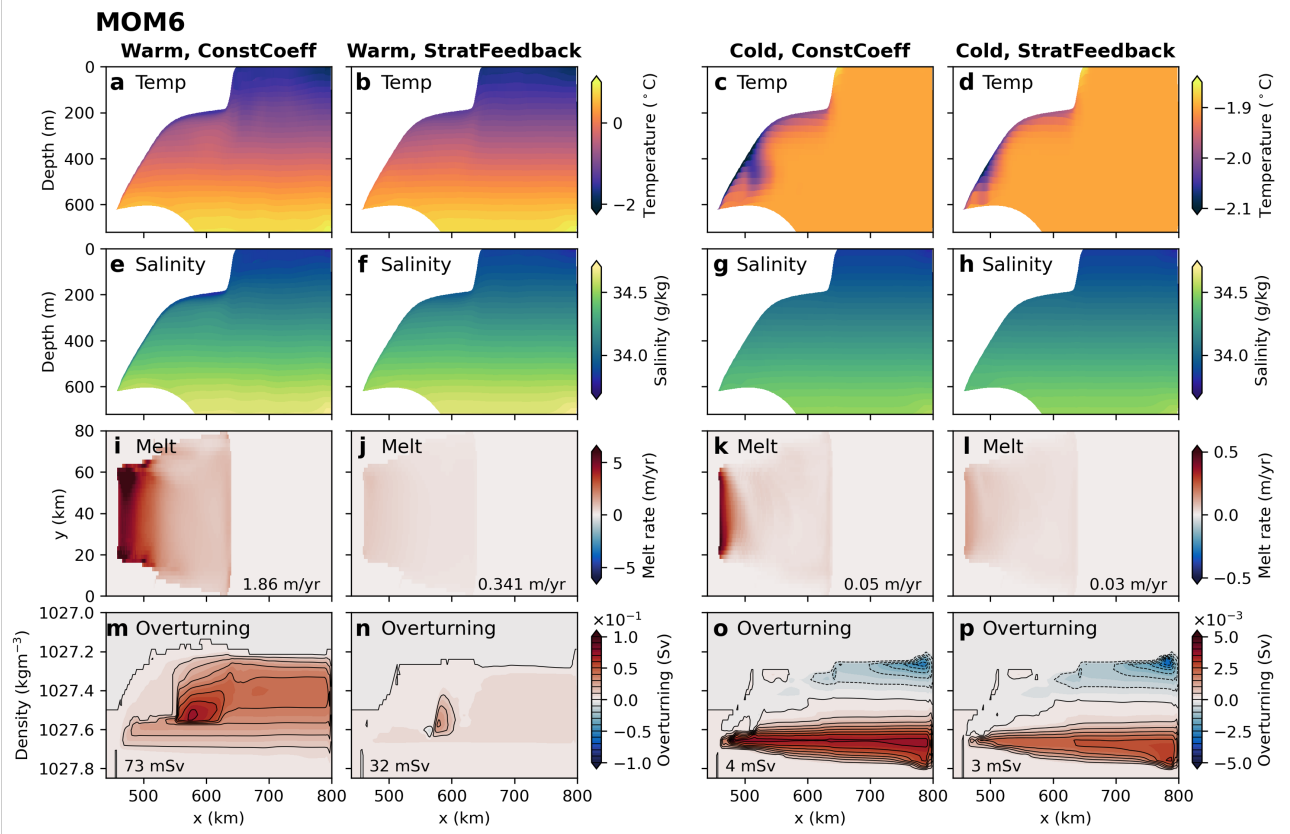

Figure R4: Temperature (a-d) and salinity (e-h) transects, melt rate distribution (i-l) and zonally averaged overturning streamfunction in density coordinates (m-p) for MOM6 simulations. All experiments use the ISOMIP+ protocol-specified tidal velocity $U_t = 0.01\mathrm{m\,s^{-1}}$ as the low-velocity limit in the melt rate parameterisation. Variables are averaged over the last 180 days of the simulation, with the temperature and salinity profiles taken at the y=40 km transect. Warm experiments are in columns 1 and 2, cold in 3 and 4. Columns 1 and 3 show the constant coefficient melt parameterisation results, and columns 2 and 4 contain the stratification feedback parameterisation. Melt rates averaged over the ice shelf are listed in panels i-l. Black contours in m-p are spaced by 10 mSv in panels (m-n) and 0.5 mSv in panels (o-p), and the text lists the maximum value of the overturning streamfunction in the domain. Note the different colourbar ranges between the warm and cold simulations. Equivalent results for MITgcm are in the Appendix C.

contour lines to make it more useful. Simply state once again to note the scale change.

We have done this (Fig. R5).

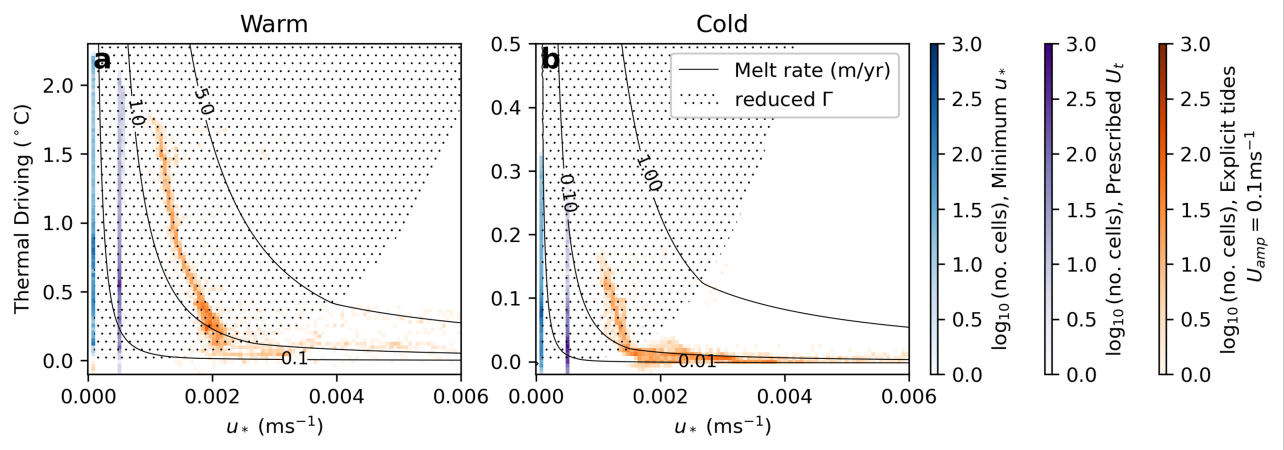

Figure R5: Thermal driving – friction velocity regime diagrams for selected MOM6 StratFeedback experiments, indicating the number of grid cells in each regime time-averaged over the final 180 days of the simulation. Panel (a) shows warm experiments and (b) cold. The minimum friction velocity $1 \times 10^{-4}\,\mathrm{m\,s^{-1}}$ experiments are shown in blue (leftmost vertical line), prescribed tidal velocity $U_t = 0.01\,\mathrm{m\,s^{-1}}$ in purple (middle vertical line) and explicit tidal forcing with amplitude $0.1\,\mathrm{m\,s^{-1}}$ in orange colours to the right. StratFeedback melt rates are shown in the solid contours and stippling shows where transfer coefficients are reduced from the ConstCoeff values, both calculated assuming a salinity $S_M = 34.05\,\mathrm{g/kg}$ and pressure 300 dbar, which are representative values for the ISOMIP+ cavity. Note the difference in y-axis extent between panels.

Revised Section 4.4

Sec 4.4: Realistic Pine Island Glacier Simulation

To assess the parameterisation in a realistic situation where circulation is more complex and the results can be compared with observations, we use the MITgcm Pine Island Glacier setup of Nakayama et al. (2021) (model details in Section 3.2) with its drag coefficient tuned to achieve melt rates similar to the Adusumilli et al. (2020) satellite melt rate product. After 20 days of simulation, area-averaged melt rates are approximately equilibrated and of a similar magnitude of ∼17 m/yr (as a result of the tuning, Table 2, noting that this rate refers to the whole simulated cavity average rather than masked tuning melt rate in Sect. 3.2). We compare the melt rate distributions for three different parameterisation choices averaged over days 20-50. The simulation run with the Holland and Jenkins (1999) parameterisation and McPhee (1981) η_* stability parameter set to 1, hereafter HJ99-neutral, requires the lowest tuning drag coefficient ($C_d = 0.004$), corresponding to the largest average melt rate if tuning is not performed (i.e. using $C_d = 0.0015$ gives an average melt rate of 11.3 m/yr, Supplementary Fig. S2a). The StratFeedback parameterisation without tuning yielded a melt rate of 4 m/yr (Fig. S2b) and required a larger tuning drag coefficient of $C_d = 0.0073$. This implies that much of the Pine Island Glacier ice shelf is in the stratified regime. Furthermore, when we include the MK18 low-velocity limit in the untuned simulations, the melt rates increase to an average of 8 m/yr (Fig. S2c). This melt rate is larger than the untuned StratFeedback simulation because

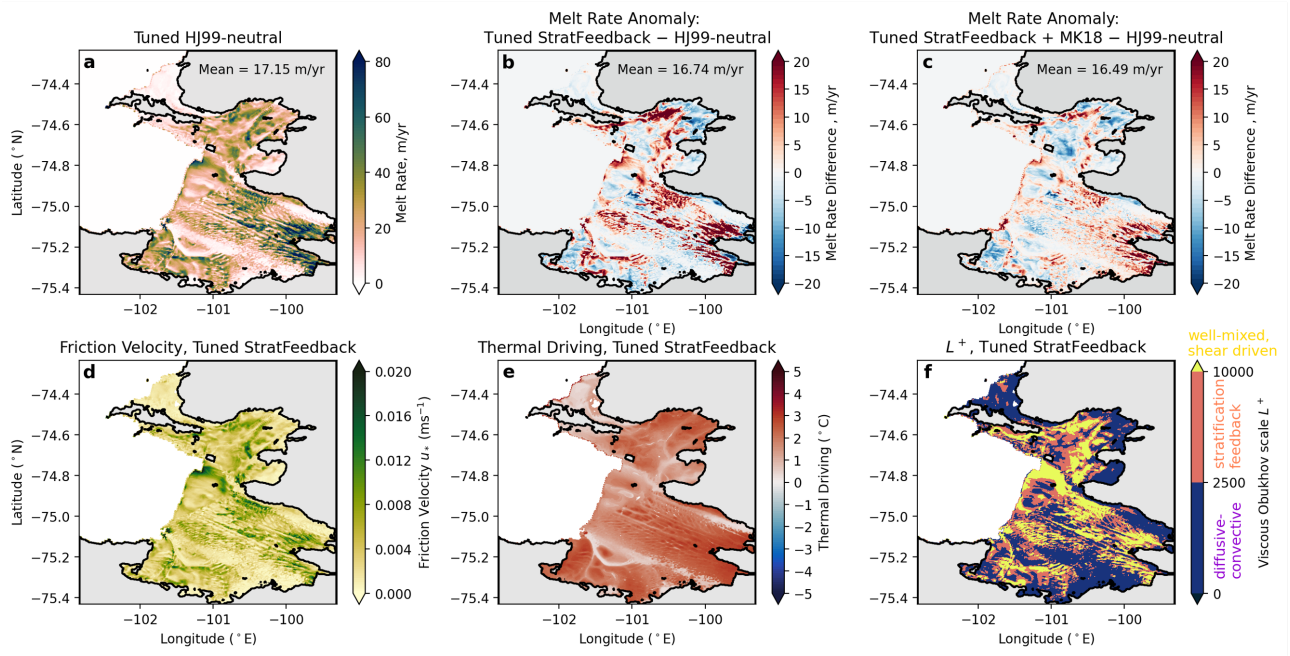

Figure R6: Fig 9: MITgcm Pine Island Glacier melt rates averaged over days 20-50 of the simulation, for (a) the tuned HJ99-neutral basal melt parameterisation used in Nakayama et al. (2021) (with a drag coefficient of $C_d = 0.004$); (b) the anomaly of the tuned stratification feedback (StratFeedback) parameterisation (with a drag coefficient of $C_d = 0.0073$) and (c) the anomaly of the tuned stratification feedback parameterisation with MK18 limit (with a drag coefficient of $C_d = 0.0057$)). Both anomalies in (b) and (c) are with respect to (a). The melt rates quoted are calculated over the whole simulated ice shelf area and differ from the tuning melt rate, which was only over the region where Adusumilli et al. (2020) data is present (Fig. D1b) and only south of 74.8°S. The friction velocity, thermal driving and viscous Obukhov scales of the stratification feedback parameterisation with tuned drag coefficient (b) are shown in panels (d), (e) and (f).

the relatively large ice base slopes (up to 30°) contribute substantial melting via the MK18 parameterisation. Because the untuned StratFeedback simulation has the weakest melting, the tuned StratFeedback simulation has the largest drag coefficient of the three tuned simulations so that the same mean melt rate is achieved. By using the tuned simulations, we can more easily compare spatial distributions of melt rate and the parameterisation's effect on ocean properties. Note the tuned drag coefficients ($C_d = 0.004$ for tuned HJ99-neutral, 0.0073 for tuned StratFeedback and 0.0057 for tuned StratFeedback+MK18) all lie between the value $C_d = 0.0015$ used in the original simulation and the value $C_d = 0.0097$ suggested by Jenkins et al. (2010) (see Sec. 2.1 for more observational estimates of drag coefficients).

In the tuned HJ99-neutral simulation, melt is enhanced near the grounding line (Fig. 9a), and reaches the observed melt rates of up to 200 m/yr in this region (Shean et al., 2019; Zinck et al., in review, see probability distribution in Fig. D1). Melt is also enhanced at the ice shelf keels (Fig. 9a), as in Shean et al. (2019). Unlike observations which suggest low melt rates in the northern part of the ice shelf, simulated melt rates reach ∼50 m/yr in this region (compare Fig. 9a and Figs. D1b,c). The difference suggests there may be differences between the simulated and real pathways of water masses into the northern section of the Pine Island Glacier ice shelf cavity.

In the tuned StratFeedback simulation, the melt rates are increased relative to the tuned

HJ99-neutral simulation in some regions, such as near the Pine Island Glacier grounding line and in the ice shelf keels (and some channels with high velocities), and decreased elsewhere (Fig. 9b). The regions where the tuned StratFeedback simulation enhances melt correspond to regions with large friction velocities (Fig. 9d) and melt decreases in regions with low friction velocities, including some regions near the grounding line. In the large friction velocity regions, L^+ is also large (Fig. 9f), indicating melting in the well-mixed regime, whereas regions with lower friction velocities have lower L^+ and are simulated to be in the stratified and diffusive-convective regimes. The StratFeedback parameterisation therefore enhances the spatial variability in melt beneath Pine Island Glacier. Ocean properties and circulation respond to this modified melt rate, leading to fresher, colder water in regions with more melting (see Supplementary Figs. S3,S4,S5).

The tuned StratFeedback+MK18 simulation has a similar melt rate anomaly pattern to the tuned StratFeedback simulation despite the different drag coefficients. However, in addition to having enhanced melt in regions with large friction velocity compared to the HJ99-neutral experiment, melt is also enhanced at the sloped ice shelf front and near the grounding line, the latter where the thermal driving is large (Fig. 9e). Both the tuned StratFeedback and StratFeedback+MK18 experiments have a larger area of the ice shelf with melting greater than 50 m/yr compared with the tuned HJ99-neutral simulation (Fig. D1), and align better with the high-resolution observational products near the grounding line (Zinck et al., in review; Shean et al., 2019). However, the missing data and coarser resolution of Adusumilli et al. (2020) make quantitative comparison challenging. Since the drag coefficient also affects the momentum equation's drag law, the less aggressive tuning required by MK18, combined with generally higher melt rates near the grounding line, indicate that the MK18 lower limit choice may be more appropriate choice. However, this assessment should be extended to other ice shelves. The general similarity between StratFeedback and StratFeedback+MK18 also indicates that large parts of the tuned Pine Island Glacier simulations are not in the low-velocity regime (with the diffusive-convective regime as a guide in Fig. 9f).

The difference in the spatial distribution of melt rates between the original simulation and that with the StratFeedback parameterisation highlights the spatial heterogeneity in melt rate regimes within individual ice shelves. All three regimes, well-mixed shear-driven, stratified and diffusive-convective, were observed in the tuned simulations (Fig. 9f). Analysis of borehole observations from Pine Island Glacier yielded a shear-driven L^+ of 1.1×10^4 (Fig. 3b), which was taken in one of the channels approximately halfway between the ice front and grounding zone (Stanton et al., 2013). Without the precise location in the ice shelf (and noting differences in time of simulation and observation), it is difficult to determine if the simulated channels' L^+ agree with the observation. However, keels and some channels are generally simulated to be in the shear-driven regime, potentially in agreement with Stanton et al. (2013). Nevertheless, the need for significantly different drag coefficients between tuned simulations demonstrates the sensitivity of regional ice shelf models' basal melting and melt regimes to parameterisations.

Appendix D1: Pine Island Glacier melt rate distributions compared to observations

Fig. D1a compares the distribution of melt rates between the three tested parameterisations, as well as melt rates computed from the Adusumilli et al. (2020) and Zinck et al. (in review) satellite-derived melt rate products. Whilst not directly comparable, due to different resolutions and ice shelf area due to missing data (e.g. at the grounding line, where the grounding line is taken from Morlighem et al. (2020), see Figs. D1b,c), the tuned StratFeedback parameterisation

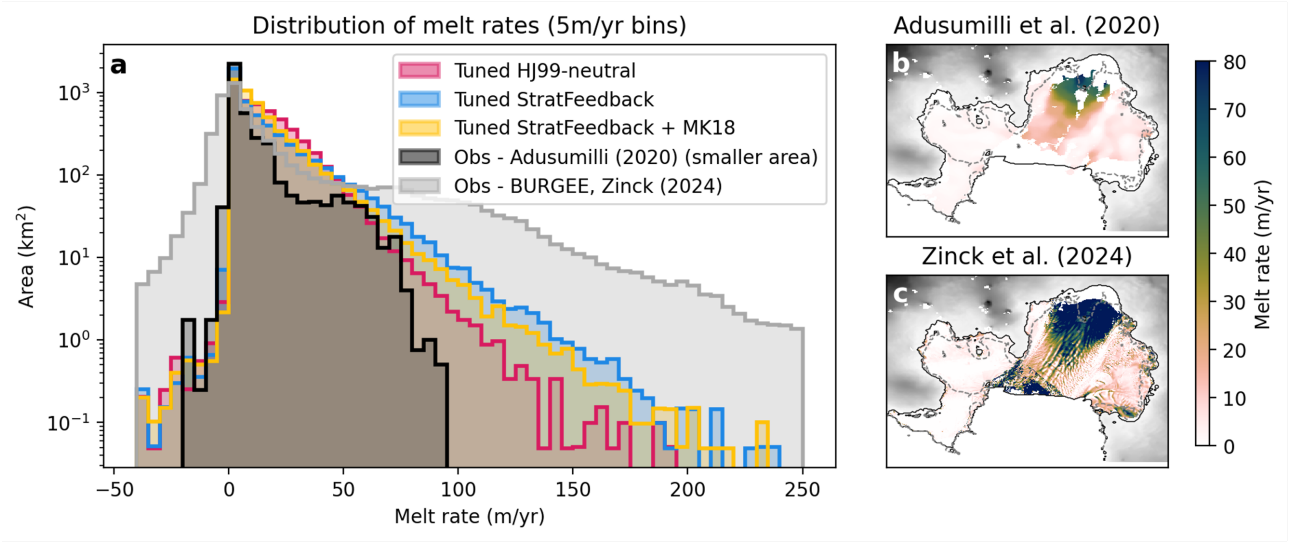

Figure R7: Fig D1: (a) Melt rate statistical distributions in Pine Island Glacier, for the MITgcm simulation with three different basal melt parameterisations compared with Adusumilli et al. (2020) (data: Adusumilli et al.) and Zinck et al. (in review) (data: Zinck et al., 2024). Note that the Adusumilli et al. (2020) product is coarser-resolution (500 m) than the MITgcm model (200 m) and is missing data whilst Zinck et al. (in review) is finer resolution (50 m). The y-axis is logarithmically scaled. MITgcm data is averaged over simulation days 20-50. (b) Adusumilli et al. (2020) melt rate and (c) Zinck et al. (in review) melt rates at Pine Island Glacier, with the same colourbar as Fig. 10a-c, but note it is rotated with the Antarctic Ice Sheet at the top of the figure and ocean at the bottom. The Bedmachine V3 surface elevation (Morlighem et al., 2020) (data: Morlighem, 2022) is shown in grey and the associated ice shelf mask is outlined with a black contour. The model domain is outlined with a grey dashed contour. Data from Adusumilli et al. is licensed under CC BY 4.0 (`https://creativecommons.org/licenses/by/4.0/`) and Zinck et al. (2024) is licensed under CC BY-SA 4.0 (`https://creativecommons.org/licenses/by-sa/4.0/`) and have been adapted in this Figure.

(blue colours) and StratFeedback+MK18 (yellow colours) have larger positive melt rate tails than the HJ99-neutral experiment (pink colours), more similar to the large ($\sim$ 200 m/yr) melt rates observed near the grounding line in high-resolution satellite products (grey colours, Zinck et al., in review), and Shean et al. (2019). Note the two satellite products here differ significantly, highlighting the uncertainty in satellite-derived melt rates. The time periods of the satellite products and model run also differ.

References

Adusumilli, S., Fricker, H. A., Medley, B. C., Padman, L., and Siegfried, M. R.: Data from: Interannual variations in meltwater input to the Southern Ocean from Antarctic ice shelves., UC San Diego Library Digital Collections., https://doi.org/10.6075/J04Q7SHT.

Adusumilli, S., Fricker, H. A., Medley, B., Padman, L., and Siegfried, M. R.: Interannual variations in meltwater input to the Southern Ocean from Antarctic ice shelves, Nature Geoscience, 13, 616–620, https://doi.org/10.1038/s41561-020-0616-z, 2020.

Alley, K. E., Scambos, T. A., Siegfried, M. R., and Fricker, H. A.: Impacts of warm water on

Antarctic ice shelf stability through basal channel formation, Nature Geoscience, 9, 290–293, https://doi.org/10.1038/ngeo2675, 2016.

Arzeno, I. B., Beardsley, R. C., Limeburner, R., Owens, B., Padman, L., Springer, S. R., Stewart, C. L., and Williams, M. J.: Ocean variability contributing to basal melt rate near the ice front of Ross Ice Shelf, Antarctica, Journal of Geophysical Research: Oceans, 119, 4214–4233, https://doi.org/10.1002/2014JC009792, 2014.

Asay-Davis, X. S., Cornford, S. L., Durand, G., Galton-Fenzi, B. K., Gladstone, R. M., Gudmundsson, G. H., Hattermann, T., Holland, D. M., Holland, D., Holland, P. R., et al.: Experimental design for three interrelated marine ice sheet and ocean model intercomparison projects: MISMIP v. 3 (MISMIP+), ISOMIP v. 2 (ISOMIP+) and MISOMIP v. 1 (MISOMIP1), Geoscientific Model Development, 9, 2471–2497, https://doi.org/10.5194/gmd-9-2471-2016, 2016.

Darelius, E., Makinson, K., Daae, K., Fer, I., Holland, P. R., and Nicholls, K. W.: Hydrography and circulation in the Filchner depression, Weddell Sea, Antarctica, Journal of Geophysical Research: Oceans, 119, 5797–5814, https://doi.org/10.1002/2014JC010225, 2014.

Davis, P. E. and Nicholls, K. W.: Turbulence observations beneath Larsen C ice shelf, Antarctica, Journal of Geophysical Research: Oceans, 124, 5529–5550, https://doi.org/10.1029/2019JC015164, 2019.

Davis, P. E., Nicholls, K. W., Holland, D. M., Schmidt, B. E., Washam, P., Riverman, K. L., Arthern, R. J., Vaňková, I., Eayrs, C., Smith, J. A., et al.: Suppressed basal melting in the eastern Thwaites Glacier grounding zone, Nature, 614, 479–485, https://doi.org/10.1038/s41586-022-05586-0, 2023.

Dutrieux, P., Stewart, C., Jenkins, A., Nicholls, K. W., Corr, H. F., Rignot, E., and Steffen, K.: Basal terraces on melting ice shelves, Geophysical Research Letters, 41, 5506–5513, https://doi.org/10.1002/2014GL060618, 2014.

Gwyther, D. E., Cougnon, E. A., Galton-Fenzi, B. K., Roberts, J. L., Hunter, J. R., and Dinniman, M. S.: Modelling the response of ice shelf basal melting to different ocean cavity environmental regimes, Annals of Glaciology, 57, 131–141, https://doi.org/10.1017/aog.2016.31, 2016.

Gwyther, D. E., Kusahara, K., Asay-Davis, X. S., Dinniman, M. S., and Galton-Fenzi, B. K.: Vertical processes and resolution impact ice shelf basal melting: A multi-model study, Ocean Modelling, 147, 101 569, https://doi.org/10.1016/j.ocemod.2020.101569, 2020.

Hellmer, H. H. and Olbers, D. J.: A two-dimensional model for the thermohaline circulation under an ice shelf, Antarctic Science, 1, 325–336, https://doi.org/10.1017/S0954102089000490, 1989.

Holland, D. M. and Jenkins, A.: Modeling thermodynamic ice–ocean interactions at the base of an ice shelf, Journal of Physical Oceanography, 29, 1787–1800, https://doi.org/10.1175/1520-0485(1999)029⟨1787:MTIOIA⟩2.0.CO;2, 1999.

Hyogo, S., Nakayama, Y., and Mensah, V.: Modeling ocean circulation and ice shelf melt in the Bellingshausen Sea, Journal of Geophysical Research: Oceans, 129, e2022JC019 275, https://doi.org/10.1029/2022JC019275, 2024.

Jenkins, A.: A simple model of the ice shelf–ocean boundary layer and current, Journal of Physical Oceanography, 46, 1785–1803, 2016.

Jenkins, A.: Shear, stability, and mixing within the ice shelf–ocean boundary current, Journal of Physical Oceanography, 51, 2129–2148, 2021.

Jenkins, A., Nicholls, K. W., and Corr, H. F.: Observation and parameterization of ablation at the base of Ronne Ice Shelf, Antarctica, Journal of Physical Oceanography, 40, 2298–2312, https://doi.org/10.1175/2010JPO4317.1, 2010.

Jordan, J. R., Holland, P. R., Jenkins, A., Piggott, M. D., and Kimura, S.: Modeling ice-ocean interaction in ice-shelf crevasses, Journal of Geophysical Research: Oceans, 119, 995–1008, https://doi.org/10.1002/2013JC009208, 2014.

Jourdain, N. C., Molines, J.-M., Le Sommer, J., Mathiot, P., Chanut, J., de Lavergne, C., and Madec, G.: Simulating or prescribing the influence of tides on the Amundsen Sea ice shelves, Ocean Modelling, 133, 44–55, https://doi.org/10.1016/j.ocemod.2018.11.001, 2019.

Kerr, R. C. and McConnochie, C. D.: Dissolution of a vertical solid surface by turbulent compositional convection, Journal of Fluid Mechanics, 765, 211–228, https://doi.org/10.1017/jfm.2014.722, 2015.

Lawrence, J., Washam, P., Stevens, C., Hulbe, C., Horgan, H., Dunbar, G., Calkin, T., Stewart, C., Robinson, N., Mullen, A., et al.: Crevasse refreezing and signatures of retreat observed at Kamb Ice Stream grounding zone, Nature Geoscience, 16, 238–243, https://doi.org//10.1038/s41561-023-01129-y, 2023.

Makinson, K., Schröder, M., and Østerhus, S.: Effect of critical latitude and seasonal stratification on tidal current profiles along Ronne Ice Front, Antarctica, Journal of Geophysical Research: Oceans, 111, https://doi.org/10.1029/2005JC003062, 2006.

Malyarenko, A., Wells, A. J., Langhorne, P. J., Robinson, N. J., Williams, M. J., and Nicholls, K. W.: A synthesis of thermodynamic ablation at ice–ocean interfaces from theory, observations and models, Ocean Modelling, 154, 101 692, https://doi.org/10.1016/j.ocemod.2020.101692, 2020.

McConnochie, C. and Kerr, R.: Testing a common ice-ocean parameterization with laboratory experiments, Journal of Geophysical Research: Oceans, 122, 5905–5915, https://doi.org/10.1002/2017JC012918, 2017.

McConnochie, C. D. and Kerr, R. C.: Dissolution of a sloping solid surface by turbulent compositional convection, Journal of Fluid Mechanics, 846, 563–577, https://doi.org/10.1017/jfm.2018.282, 2018.

McPhee, M.: Air-ice-ocean interaction: Turbulent ocean boundary layer exchange processes, Springer Science & Business Media, 2008.

McPhee, M. G.: An analytic similarity theory for the planetary boundary layer stabilized by surface buoyancy, Boundary-Layer Meteorology, 21, 325–339, https://doi.org/10.1007/BF00119277, 1981.

McPhee, M. G., Maykut, G. A., and Morison, J. H.: Dynamics and thermodynamics of the ice/upper ocean system in the marginal ice zone of the Greenland Sea, Journal of Geophysical Research: Oceans, 92, 7017–7031, https://doi.org/10.1029/JC092iC07p07017, 1987.

Morlighem, M.: MEaSUREs BedMachine Antarctica, Version 3., https://doi.org/10.5067/FPSU0V1MWUB6, accessed 22 October 2024, 2022.

Morlighem, M., Rignot, E., Binder, T., Blankenship, D., Drews, R., Eagles, G., Eisen, O., Ferraccioli, F., Forsberg, R., Fretwell, P., et al.: Deep glacial troughs and stabilizing ridges

unveiled beneath the margins of the Antarctic ice sheet, Nature Geoscience, 13, 132–137, https://doi.org/10.1038/s41561-019-0510-8, 2020.

Mueller, R., Padman, L., Dinniman, M. S., Erofeeva, S., Fricker, H. A., and King, M.: Impact of tide-topography interactions on basal melting of Larsen C Ice Shelf, Antarctica, Journal of Geophysical Research: Oceans, 117, https://doi.org/10.1029/2011JC007263, 2012.

Nakayama, Y., Menemenlis, D., Zhang, H., Schodlok, M., and Rignot, E.: Origin of Circumpolar Deep Water intruding onto the Amundsen and Bellingshausen Sea continental shelves, Nature Communications, 9, 1–9, https://doi.org/10.1038/s41467-018-05813-1, 2018.

Nakayama, Y., Manucharyan, G., Zhang, H., Dutrieux, P., Torres, H. S., Klein, P., Seroussi, H., Schodlok, M., Rignot, E., and Menemenlis, D.: Pathways of ocean heat towards Pine Island and Thwaites grounding lines, Scientific Reports, 9, 16 649, https://doi.org/10.1038/s41598-019-53190-6, 2019.

Nakayama, Y., Cai, C., and Seroussi, H.: Impact of subglacial freshwater discharge on Pine Island Ice Shelf, Geophysical Research Letters, 48, e2021GL093 923, https://doi.org/10.1029/2021GL093923, 2021.

Nicholls, K., Abrahamsen, E., Buck, J., Dodd, P., Goldblatt, C., Griffiths, G., Heywood, K., Hughes, N., Kaletzky, A., Lane-Serff, G., et al.: Measurements beneath an Antarctic ice shelf using an autonomous underwater vehicle, Geophysical Research Letters, 33, https://doi.org/10.1029/2006GL025998, 2006.

Nicholls, K. W., Makinson, K., and Østerhus, S.: Circulation and water masses beneath the northern Ronne Ice Shelf, Antarctica, Journal of Geophysical Research: Oceans, 109, https://doi.org/10.1029/2004JC002302, 2004.

Orlanski, I.: A simple boundary condition for unbounded hyperbolic flows, Journal of Computational Physics, 21, 251–269, https://doi.org/10.1016/0021-9991(76)90023-1, 1976.

Paolo, F. S., Fricker, H. A., and Padman, L.: Volume loss from Antarctic ice shelves is accelerating, Science, 348, 327–331, https://doi.org/10.1126/science.aaa0940, 2015.

Pope, S. B.: Turbulent flows, Measurement Science and Technology, 12, 2020–2021, 2001.

Rignot, E., Mouginot, J., Scheuchl, B., Van Den Broeke, M., Van Wessem, M. J., and Morlighem, M.: Four decades of Antarctic Ice Sheet mass balance from 1979–2017, Proceedings of the National Academy of Sciences, 116, 1095–1103, https://doi.org/10.1073/pnas.1812883116, 2019.

Rosevear, M. G., Galton-Fenzi, B., and Stevens, C.: Evaluation of basal melting parameterisations using in situ ocean and melting observations from the Amery Ice Shelf, East Antarctica, Ocean Science, 18, 1109–1130, https://doi.org/0.5194/os-18-1109-2022, 2022a.

Rosevear, M. G., Gayen, B., and Galton-Fenzi, B. K.: Regimes and transitions in the basal melting of Antarctic ice shelves, Journal of Physical Oceanography, 52, 2589–2608, https://doi.org/10.1175/JPO-D-21-0317.1, 2022b.

Rosevear, M. G., Gayen, B., Vreugdenhil, C. A., and Galton-Fenzi, B. K.: How Does the Ocean Melt Antarctic Ice Shelves?, Annual Review of Marine Science, 17, https://doi.org/10.1146/annurev-marine-040323-074354, 2024.

Schmidt, B. E., Washam, P., Davis, P. E., Nicholls, K. W., Holland, D. M., Lawrence, J. D., Riverman, K. L., Smith, J. A., Spears, A., Dichek, D., et al.: Heterogeneous

melting near the Thwaites Glacier grounding line, Nature, 614, 471–478, https://doi.org/10.1038/s41586-022-05691-0, 2023.

Schulz, K., Nguyen, A., and Pillar, H.: An Improved and Observationally-Constrained Melt Rate Parameterization for Vertical Ice Fronts of Marine Terminating Glaciers, Geophysical Research Letters, 49, e2022GL100 654, https://doi.org/10.1029/2022GL100654, 2022.

Shean, D. E., Joughin, I. R., Dutrieux, P., Smith, B. E., and Berthier, E.: Ice shelf basal melt rates from a high-resolution digital elevation model (DEM) record for Pine Island Glacier, Antarctica, The Cryosphere, 13, 2633–2656, https://doi.org/10.5194/tc-13-2633-2019, 2019.

Shrestha, K., Manucharyan, G. E., and Nakayama, Y.: Submesoscale variability and basal melting in ice shelf cavities of the Amundsen Sea, Geophysical Research Letters, 51, e2023GL107 029, https://doi.org/10.1029/2023GL107029, 2024.

Stanton, T. P., Shaw, W., Truffer, M., Corr, H., Peters, L., Riverman, K., Bindschadler, R., Holland, D., and Anandakrishnan, S.: Channelized ice melting in the ocean boundary layer beneath Pine Island Glacier, Antarctica, Science, 341, 1236–1239, https://doi.org/10.1126/science.1239373, 2013.

Stewart, C. L.: Ice-ocean interactions beneath the north-western Ross Ice Shelf, Antarctica, Ph.D. thesis, https://doi.org/10.17863/CAM.21483, 2018.

Vreugdenhil, C. A. and Taylor, J. R.: Stratification effects in the turbulent boundary layer beneath a melting ice shelf: Insights from resolved large-eddy simulations, Journal of Physical Oceanography, 49, 1905–1925, https://doi.org/10.1175/JPO-D-18-0252.1, 2019.

Wåhlin, A., Alley, K. E., Begeman, C., Hegrenæs, Ø., Yuan, X., Graham, A. G., Hogan, K., Davis, P. E., Dotto, T. S., Eayrs, C., et al.: Swirls and scoops: Ice base melt revealed by multibeam imagery of an Antarctic ice shelf, Science Advances, 10, eadn9188, https://doi.org/10.1126/sciadv.adn9188, 2024.

Washam, P., Nicholls, K. W., Münchow, A., and Padman, L.: Tidal modulation of buoyant flow and basal melt beneath Petermann Gletscher Ice Shelf, Greenland, Journal of Geophysical Research: Oceans, 125, e2020JC016 427, https://doi.org/10.1029/2020JC016427, 2020.

Washam, P., Lawrence, J. D., Stevens, C. L., Hulbe, C. L., Horgan, H. J., Robinson, N. J., Stewart, C. L., Spears, A., Quartini, E., Hurwitz, B., et al.: Direct observations of melting, freezing, and ocean circulation in an ice shelf basal crevasse, Science Advances, 9, eadi7638, https://doi.org/10.1126/sciadv.adi7638, 2023.

Watkins, R. H., Bassis, J. N., and Thouless, M.: Roughness of ice shelves is correlated with basal melt rates, Geophysical Research Letters, 48, e2021GL094 743, https://doi.org/10.1029/2021GL094743, 2021.

Wilson, N. J., Vreugdenhil, C. A., Gayen, B., and Hester, E. W.: Double-Diffusive Layer and Meltwater Plume Effects on Ice Face Scalloping in Phase-Change Simulations, Geophysical Research Letters, 50, e2023GL104 396, https://doi.org/10.1029/2023GL104396, 2023.

Wiskandt, J. and Jourdain, N.: Brief Communication: Representation of heat conduction into the ice in marine ice shelf melt modeling, EGUsphere, 2024, 1–10, https://doi.org/10.5194/egusphere-2024-2239, in review.

Zhao, K. X., Skyllingstad, E. D., and Nash, J. D.: Improved parameterizations of vertical ice-ocean boundary layers and melt rates, Geophysical Research Letters, 51, e2023GL105 862, https://doi.org/10.1029/2023GL105862, 2024.

Zhou, Q. and Hattermann, T.: Modeling ice shelf cavities in the unstructured-grid, Finite Volume Community Ocean Model: Implementation and effects of resolving small-scale topography, Ocean Modelling, 146, 101 536, 2020.

Zinck, A.-S. P., Lhermitte, S., Wearing, M., and Wouters, B.: Dataset belonging to the article: Exposure to Underestimated Channelized Melt in Antarctic Ice Shelves, https://doi.org/10.4121/4e2ba9a9-7b1b-4837-b52d-036f8c876e67.v1, 2024.

Zinck, A.-S. P., Lhermitte, S., Wearing, M., and Wouters, B.: Exposure to Underestimated Channelized Melt in Antarctic Ice Shelves, https://doi.org/10.21203/rs.3.rs-4806463/v1, in review.